

PAPER • OPEN ACCESS

Using the Robust High Density-surface Electromyography Features for Real-Time Hand Gestures Classification

To cite this article: Hanadi A Jaber *et al* 2020 *IOP Conf. Ser.: Mater. Sci. Eng.* **745** 012020

View the [article online](#) for updates and enhancements.

Using the Robust High Density-surface Electromyography Features for Real-Time Hand Gestures Classification

Hanadi A Jaber¹, Mofeed T Rashid² and L Fortuna³

¹ Computer Engineering Department, University of Basrah, Basrah, Iraq (hanadyce@gmail.com).

² Electrical Engineering Department, University of Basrah, Basrah, Iraq (Mofeed.t.rashid@ieee.org).

³ Dipartimento di Ingegneria Elettrica Elettronica, Informatica, Università degli Studi di Catania, Catania, Italy.

Abstract. Using High-Density surface Electromyography (HD-sEMG) signals for gesture classification has augmented the spatial information of muscle activity by increasing the density and convergence of the electrodes. In this paper, spatial features are extracted from HD-sEMG data. These features generated by combining HOG features of HD-sEMG map and intensity features calculated from the average of segmented HD-sEMG map which is denoted as (AIH) features. Real-time evaluation was performed for inter-session identification. The simulation of proposed algorithms is achieved by MATLAB; the result of our experiments achieves high accuracy with good performance based on spatial features reached to 99%. The comparison of our results with other research indicates that the proposed algorithms can enhance the performance and accuracy of gestures identification process by SVM classifier. In addition, the results confirm the robustness of the spatial features to the variation of EMG signals over time.

1. Introduction

Electromyography (EMG) signal is a neural control for recognizing human intent motion that generated during muscle contraction. EMG signals among other bioelectric signals had a problem of analyzing due to its stochastic and non-stationary properties. The myoelectric control system uses EMG signals as a control input to perform prosthetic functions. These prostheses increase the abilities of amputees and other patients with physical damage or cognitive functions result from disease, injury, and aging [1,2].

The myoelectric control system is divided into two categories: conventional control system and pattern recognition approach. The conventional control system uses the amplitude of each pair of electrode site controls one motion of the prostheses. While the pattern recognition approach augments the number of degrees of freedom (DOF) that can be intuitively controlled [3-6]. Myoelectric pattern recognition has been used for different applications such as prostheses [7-9], wheelchairs [10], rehabilitation robots [11].

Typically, there are two techniques to recording EMG signals, either sparse electrodes that required precise position over the muscle area or single array that position at the circumference of a specific area such as Armband. Electrodes organized in two-dimensional array of closely spaced electrodes that covered a limited muscle known as HD-sEMG. The number of electrodes utilized for HD-sEMG data ranges from 35 to over 350 while the largest number of Armband electrodes is 16 [6,12].



HD-sEMG signals have been analyzed using two methods. One known as HD-sEMG map [13] and instantaneous image [14]. HD-sEMG map is an image formulation obtained from signal amplitude for specific time window of raw sEMG signals. Sometimes it is called intensity or heat map. Instantaneous images organized directly from raw sEMG signals. The number of image pixels corresponds to the number of electrodes for example if HD-sEMG signals arranged in 8×16 electrodes then the instantaneous image forms with 8×16 pixels. Accordingly, the number of instantaneous images constrained to sampling rate (e.g. if sampling frequency 1kHz and muscle contraction consists of 3s, then the number of instantaneous images was 3000). HD-sEMG data enable new possibility to use the EMG signals for image processing techniques. Jordanic et al. [15] employed HD-sEMG map to extract spatial features using mean shift channel algorithm combined with an intensity features to recognize twelve movement classes corresponding to four motion types with three effort levels. Its classifier achieved the highest performance during fatigue and long-term identification. Stango [16] used HD-sEMG signals for controlling upper prostheses; robust features were used to reduce the effect of electrode number and shift that influenced the robustness and reliability of myoelectric pattern recognition during donning and doffing the prosthesis. His results achieved 95% classification accuracy. Geng et al. [14] proposed instantaneous recording of HD-sEMG as an image. The researchers implemented deep learning represented by convolution neural network for gesture identification. The highest recognition accuracy was obtained by simple majority voting algorithm over 150 frames reached 99%. Consequently Du et al. [17] used the same method of [14] but with adaptation to investigate higher performance for inter-session and inter-subject strategies. Roberto [18] used instantaneous images such that each pixel corresponds to instantaneous sample of EMG channels. Feature extracted after divide image into blocks. His results achieved accuracy reach to 91%. Amma [19] used spatial features and HD-sEMG map to reduce the changes of EMG signal over time and electrode shift to achieved classification accuracy to recognize 27 gestures. Our previous work [21] used envelop of HD-sEMG signals and extract the AIH features from HD-sEMG map. Our results achieved higher performance for three sub-databases compared with SVM performance based on TD features.

In this paper, AIH features were extracted from HD-sEMG map by combining the HOG features of RMS-map and intensity of average segmented map per channel. Our experiment extended to implement real-time evaluation for inter-session identification. Results ensure the robustness of our feature set to the variation of EMG signals over time and between the sessions.

The rest of the paper is organized as follows: Section 2 gives a description of gesture recognition as well as the requirements for this task. Section 3 tackles the simulation of the SVM classifier by MATLAB performed in order to test the accuracy of HD-sEMG features extraction algorithm. The final section contains the conclusions.

2. EMG pattern Recognition

2.1. Experimental Database

The HD-sEMG data of our experiments was obtained from CapgMyo standard database [20] which is used in [14,17,18]. A wearable non-invasive device was used to acquire HD-sEMG data. It consists of 128 channels prepared in quadrature grid of 8×16 electrodes. EMG signals sampled at 1kHz and pre-processed using band-pass filtered at 20-380 Hz. CapgMyo database contains three sub-databases; DB-a consists of 18 healthy able-bodied subjects. Each subject performed eight isometric hand gestures. Each gesture repeated for 10 trials. DB-b includes the same gestures of DB-a but acquired from 10 subjects recorded in two sessions for different days. DB-c contains 12 gestures acquired from 10 subjects. The gestures implemented in our experiments are shown in Figure 1. In other word, these gestures correspond to DB-a and DB-b.

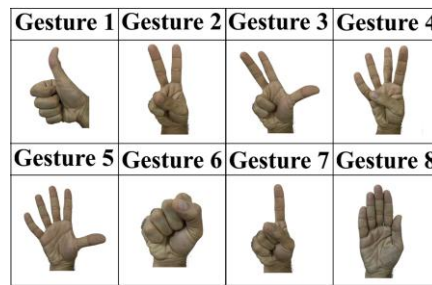


Figure 1. Hand gestures configurations.

2.2. HD-sEMG Signal Analysis

Robustness of prosthesis control system depends on employing HD-sEMG electrodes to get more information and discover invariant characteristics of EMG signals. The development of HD-sEMG signals augment the data size significantly and introduced the possibility of using EMG image.

There are two methods for analyzing HD-sEMG signals; HD-sEMG map and instantaneous image. In this work, HD-sEMG map is used. Consequently, the recorded data for each channel is divided into non-overlapping windows. HD-sEMG map is calculated using root mean square (RMS) for each window as a segmented map [13,22].

$$SM_{i,j} = \sqrt{\frac{1}{N} \sum_{n=0}^{N-1} EMG_{i,j}^2} \quad (1)$$

Where N denotes samples number f segmented window, $SM_{i,j}$ is HD-sEMG map of the segmented window, $EMG_{i,j}$ corresponds to recorded EMG signals at (i,j) channel. The average map is obtained by averaging segmented map at each channel as

$$AM_{i,j} = \frac{1}{M} \sum_{m=0}^M SM_{i,j} \quad (2)$$

where $AM_{i,j}$ is the average value of segmented map located at (i,j) channel and denoted as an average map, M denote the window's number. Average map considered as an image in which each pixel corresponds to channel. Consequently, the average map is used as the input to the feature extraction method.

2.3. Features Extraction

Different algorithms have employed to extract features from the EMG signal, some of them are simple and depend on RMS value to estimate EMG amplitude, others use time-domain features (TD). Time is the favorite domain due to the simplicity of computation with good performance and can be supported by other features in order to enhance the classifier performance [23]. More complex algorithm that depends on frequency features such as Fourier and wavelet domain [24]. New studies display that the spatial distribution of HD-sEMG maps improves the recognition of gestures [13,16]. Consequently, the spatial features of HD-sEMG maps are used either individually or combined to improve their performance [15].

In this study, AIH feature extraction is implemented. H features related to HOG features of an average map that considered as an image. Its size corresponds to electrodes locations. The intensity features I are calculated for segmented maps after averaged per channel. Consequently, vector of 1×128 features are obtained. Intensity features are calculated as logarithm of segmented maps as

$$I = \log_{10} \sum_{i,j} ASM_{i,j} \quad (3)$$

where ASM is the average of segmented maps per channel.

The average intensity vector (AI) combined with H features to form AIH features. The block diagram of the proposal feature set illustrated is in Figure 2.

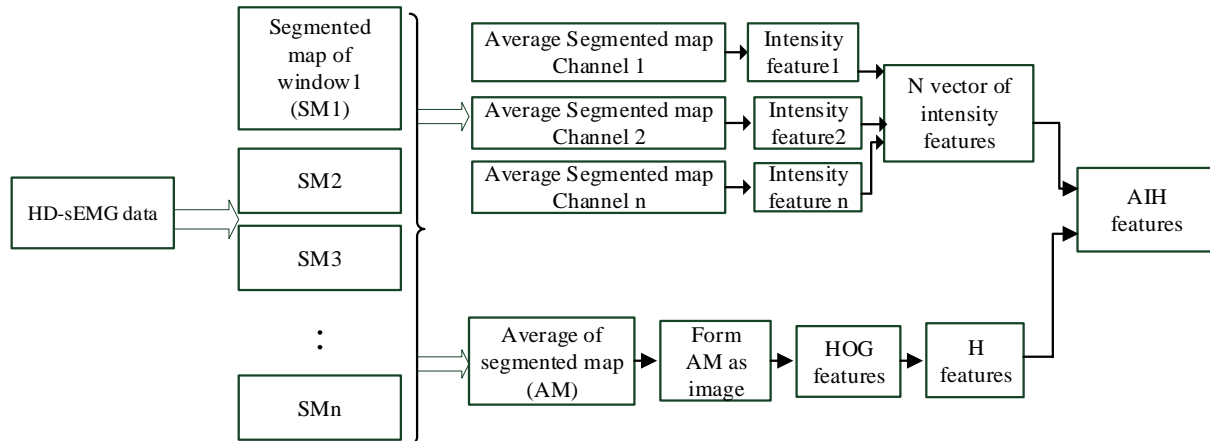


Figure 2. The block diagram of AIH features extraction approach.

2.4. SVM classifier

Many researchers use the SVM classifier because of its simplicity, solid formulation, fast training and good classification performance for small training sets.

Let dataset $D = \{(x_1, y_1), \dots, (x_n, y_n)\}$, where $x_i \in \mathfrak{R}$ is the i^{th} training vector, $y_i = \pm 1$ is a corresponding class label. The SVM classifier of the form $f(x) = w^T \phi(x) + b$, obtained by minimizing

$$\min_{w, b, \xi} \frac{1}{2} \|w\|^2 + C \sum_{i=1}^n \xi_i \quad (4)$$

subject to the constrains

$$y_i [w^T \phi(x_i) + b] \geq 1 - \xi_i \quad \forall i \in \{1, \dots, n\}$$

$$\xi_i \geq 0 \quad \forall i \in \{1, \dots, n\}$$

where $b \in \mathfrak{R}$ is the bias, $w \in \mathfrak{R}$ are the weights, ξ_i training error of x_i and C is the regularization parameter.

The performance of SVM classifier was evaluated offline in term of Sensitivity, Precision, and Accuracy for each gesture based on confusion matrix

$$S = \frac{TP}{TP + FN} \quad (5)$$

$$P = \frac{TP}{TP + FP} \quad (6)$$

$$A_{cc} = \frac{TP + TN}{TP + TN + FP + FN} \quad (7)$$

where TP (true positive) is the number of samples of a specific class that classified properly and TN (true negative) is the number of samples that do not belong to a specific class and not related to that class. FN (false negative) is the number of samples pertaining to a specific class but erroneously classified into another class, and FP (false positive) is the number of samples that are not pertaining to a definite class but incorrectly classified into that class [13,21,22].

For online evaluation, the performance is evaluated in term of overall classification accuracy for each

testing cycle as

$$CA \% = \frac{\text{number of correct predicted samples}}{\text{total test samples}} \times 100 \quad (8)$$

3. Simulation Results

In this paper, two sets of experiments are conducted in order to test the powerful of AIH features for offline and online evaluation

3.1. Offline evaluation

In this part, the experiment of our previous work [22] was re-evaluated to include all able-bodied subjects of database DB-a with different evaluations to be familiar with other researchers to compare with them. Therefore, for each subject, the classifier is trained by five trials and tested on the remaining five trails (50% training set, 50% testing set). Table 1 shows the performance of SVM classifier based on AIH features for 18 subjects.

TABLE 1. The accuracy, precision, and sensitivity of eighteen-subjects of SVM classifier using AIH features

Subjects	Accuracy%	Precision%	Sensitivity %
Sub1	100	100	100
Sub2	99.375	97.9	97.5
Sub3	98.12	93.3	92.5
Sub4	100	100	100
Sub5	99.37	97.9	97.5
Sub6	98.75	95.8	95
Sub7	98.125	92.3	92.5
Sub8	98.75	95.8	95
Sub9	100	100	100
Sub10	98.5	96.4	95
Sub11	100	100	100
Sub12	100	100	100
Sub13	99.37	97.9	97.5
Sub14	97.5	93.2	90
Sub15	100	100	100
Sub16	98.12	94.3	92.5
Sub17	100	100	100
Sub18	97.5	93.2	90
Average	99.08	97.1	96.38

It is noticed that the SVM classifier based on AIH features achieved higher performance for all subjects averaged between eight gestures. The worst subject investigates the recognition performance with 97.5% (Accuracy), 93.2% (Precision) and 90% (Sensitivity), which is an accurate performance. The average accuracy of 18 subjects reached 99%. This shows the possibility of AIH features to classify eight gestures using simple classifier trained by small training set. Accordingly, our results confirm that the choice of features was more important than the choice of classifier. Moreover, we can see that the performance of each gesture averaged between 18 subjects was investigate good performance above Precision 91.7 % and Sensitivity 86.6% as shown in Figure 3. It can be observed that most gestures produced higher recognition performance except gesture4 and gesture5, which is, still provides acceptable performance. The classification performance of gestures in terms of precision and sensitivity showed the efficient of AIH features for recognition.

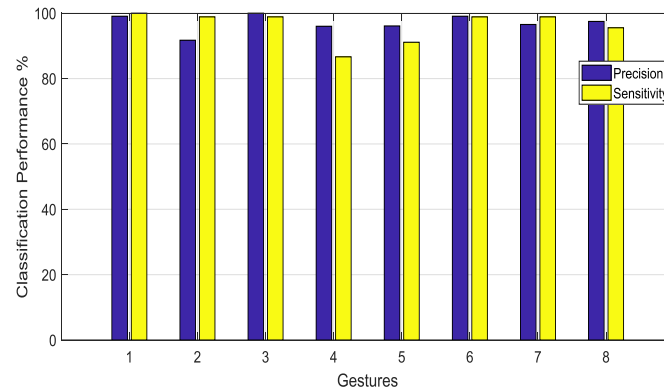


Figure. 3 The classification performance based on the precision and sensitivity of eight gestures averaged between 18 subjects

The proposed method compared with other researchers that used HD-sEMG data. Jordanic [15] used HD-sEMG map and spatial features using mean shift channel algorithm combined with intensity features. Jordanic used three HD-sEMG maps associated with three arrays of HD-sEMG signal. Accordingly, scalar intensity value was calculated for each map as a logarithm of summation of all HD-sEMG map elements. While in our method the intensity features calculated from average maps obtained from five frames per channel. As a result, the size of intensity features is related to the number of electrodes (i.e. in our method, the size of intensity features was 128). In [17] use the same databases and powerful of deep learning to attain higher accuracy reached 99.5 % using instantaneous image of recorded HD-sEMG signals. The majority voting of 150 frames was used to achieve this accuracy. While our method used simple classifier that required small training set compared with large data sets required by deep learning to achieve average accuracy reached 99%. This confirms that the choice of features is significantly affect the performance of recognition. Moreover, our study also compared with the previous work [18], which used instantaneous image for analyzing HD-sEMG data, instantaneous image, divided into blocks for three scenarios that two blocks image give best result than others. We extend our experiment to be the same evaluation procedure as [18]. The same databases have been used (i.e. sub-database DB-a) which, the comparison illustrated in Table 2. It can be noticed that our method superior to the latest work in all performance parameters [18]. The improvement of TPR reach 5% than [18], precision improved by 5.8% and F. score improvement by 4.4%.

Table 2. Comparison of our work with previous work [18]

Gestures	Roberto [18]				Our work			
	TPR	FPR	Pr.	Fsc.	TPR	FPR	Pr.	Fsc.
G1	0.955	0.009	0.938	0.946	1	0.001	0.99	0.994
G2	0.924	0.015	0.895	0.909	0.988	0.017	0.917	0.944
G3	0.898	0.013	0.909	0.930	0.988	0	100	0.993
G4	0.898	0.026	0.828	0.846	0.866	0.006	0.96	0.887
G5	0.901	0.010	0.927	0.914	0.911	0.006	0.96	0.923
G6	0.967	0.004	0.975	0.971	0.988	0.001	0.99	0.988
G7	0.949	0.011	0.926	0.937	0.988	0.006	0.965	0.974
G8	0.834	0.013	0.899	0.865	0.955	0.004	0.974	0.961
Aver.	0.911	0.012	0.912	0.914	0.961	0.005	0.97	0.958

TPP: True positive rate, FPR: False positive rate, Pr.: precision, Fsc.: F1 score

3.2. Online evaluation

Typically, poor performance has been obtained when training on the session and evaluating on others that there is a contrast of distribution of the training and testing data between sessions due to the nonstationary property of EMG signal over time and the variation of electrodes positions between sessions. Accordingly, the performance of inter-session identification deteriorates over time. To overcome this problem, either select efficient training protocols, choose robust features set or using adaptive learning method. This part shows the effectiveness of the proposed method for inter-session performance. The sub-database DB-b was applied which it contains ten subjects participate in two sessions on two different days. With a view of reducing the significant distribution of data between sessions, SVM classifier was trained by session1 and only two trails of session2 and evaluated by the remaining samples of session2. The testing data divided into streams that come simultaneously on the remaining trails of session2. Each stream has the same number of samples as shown in Figure 4.

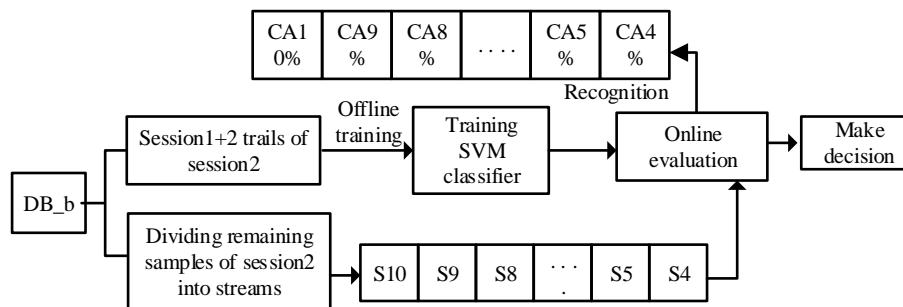


Figure 4. Block diagram of online evaluation of SVM classifier

The classification accuracy (CA%) was calculated for each testing stream. The performance of an online classifier based on AIH features for four subjects with their average accuracy are shown in Figure 5. It can be noticed that the online evaluation is achieved higher classification accuracy in term of inter-session identification. The average classification accuracy produced an acceptable performance above 87.5 %. However, this reveals the robustness of AIH features to predict the gestures for eight batches online.

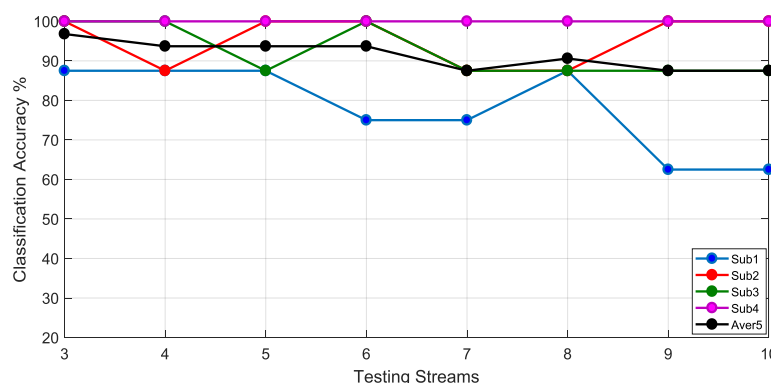


Figure 5. Online evaluation of SVM classifier for four subjects with their averaged for inter-session classification.

The inter-session performance of ten subjects of DB-b in terms of accuracy, precision, and sensitivity was shown in Figure 6. It is observed that SVM classifier based on AIH features achieved good results

for all subjects above 85% except subject1. However, it achieved acceptable performance. This confirms the robustness of AIH features to encounter the nonstationary characteristics of EMG signals over time with good performance for ten subjects participated in two sessions.

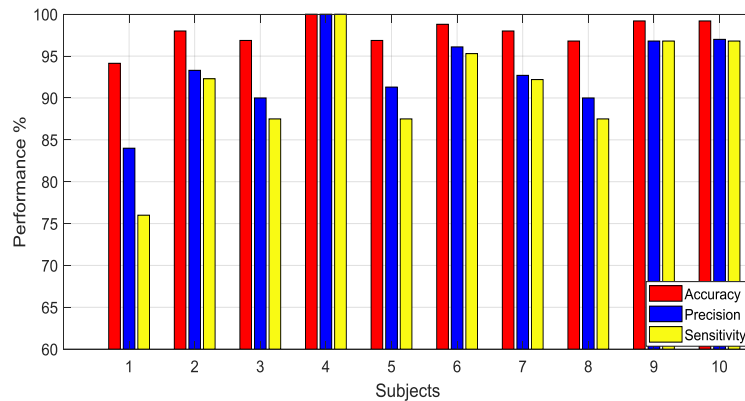


Figure. 6 The classification performance for inter-session identification

4. Conclusion

The variation of EMG signals caused a big challenging that constrains the commercialization of upper limb devices. In this paper, spatial features are extracted from HD-sEMG data. These features concerned with HOG features and intensity features averaged between windowed HD-sEMG map. The offline evaluation achieved higher performance in terms of accuracy, precision, and sensitivity to classify eight gestures based on 18 subjects. The online evaluation reported the robustness of AIH features to electrode shift and slow changes of EMG signals over time. The spatial features were considerably improved the classification of motion intents.

References

- [1] P M Pilarski, M R Dawson and T Degris, 2013, "Adaptive artificial limbs, A real time approach to prediction and anticipation", *IEEE Robot and Automation Magazine*, vol. 20, issue(1), pp 53-64.
- [2] N Meselmani, M Khrayzat, K Chahine, 2016, "Pattern recognition of EMG signals: towards adaptive control of Robotic Arm", *IEEE Int. Multidisciplinary Conf. on Eng. Tech.*
- [3] A L Edward, M R Dawson, J S Hebert and C sherstan, 2015, "Application of real time machine learning to myoelectric prostheses control: A case series in adaptive switching", *ISPO*, vol.40, issue (5), pp 573-581.
- [4] D Farina, N Jiang, H Rehbaum, 2014, "The extraction of neural information from surface EMG for the control of upper limb prosthesis Emerging and challenging", *IEEE Trans. Neural Syst. Rehabil. Eng.*, vol. 22, pp 797- 808.
- [5] W Wei, Y Wong, Y Du, Y Hu, M Kankanhalli, W Geng, 2017, "A multi-stream convolutional neural network for sEMG-based gesture recognition in muscle-computer interface", *Pattern Recognition Letters*, vol. 119, pp 131-138.
- [6] A Phinyomark and E Scheme, 2018, "EMG pattern recognition in the era of big data and deep learning", *Big Data Cogn. Comput. MDPI*, vol. 2, issue 3.
- [7] Scheme E and Englehart KB, 2011, "Electromyogram pattern recognition for control of powered upper-limb prostheses: State of the art and challenges for clinical use", *J Rehab. Res. Dev.*, vol. 48, pp 643–659.
- [8] Vidovic M M C, Hwang H, Amsuss S, Hahne J M, Farina D and Muller K R, 2016, "Improving the robustness of myoelectric pattern recognition for upper limb prostheses by covariate shift adaptation", *IEEE Trans. Neural Syst. Rehab. ng.*, vol. 24, pp. 961–970.

- [9] Liu M, Zhang F and Huang H, 2017, "An adaptive classification strategy for reliable locomotion mode recognition", *Sensors, MDPI*, vol. 17, issue (9).
- [10] Z Alhakem and R Ali, 2019, "Fast channel selection method using crow search algorithm", *ACM Int. Conf. Proc. Series*.
- [11] Dawson MR, Sherstan C, Carey JP, Hebert JS and Pilarski PM. 2014, "Development of the Bento Arm: An improved robotic arm for myoelectric training and research", *Myoelectric Control Sympo. Fredericton, NB*, pp. 60–64.
- [12] A Phukpattaranont and P Limsakul, 2012, "Feature reduction and selection for EMG signal classification", *Expert Syst. Appl.*, vol. 39, pp. 7420–7431.
- [13] M Rojas Martínez, M A Mañanas, J F. Alonso and R. Merletti, 2013, "Identification of isometric contractions based on high density EMG maps", *J. of Electromyography and Kinesiology*, vol. 23, pp. 33-42.
- [14] Geng W, Du Y, Jin W, Wei W, Hu Y and Li J, 2016, "Gesture recognition by instantaneous surface EMG images" *Sci. Rep.*, vol. 6.
- [15] M. Jordanic, M. Rojas, M. A. Mananas, J. F. Alonso, 2017, "A novel spatial features for the identification of motor tasks using HD-EMG" *Sensors*, vol. 17.
- [16] Stango, F Negro and D Farina, 2015, "Spatial correlation of high density EMG signals provided features robust to electrode number shift in pattern recognition for Myo control", *IEEE Trans. Neural Syst. Rehabil. Eng.*, vol. 23, pp. 189-198.
- [17] Y D Wenguang, Y Hu and W Geng, 2017, "Surface EMG – based inter-session gesture recognition enhanced by Deep domain an adaptation", *Sensors*, vol. 17.
- [18] R D Amador, C A F Riesgo, J V L Ginori 2019, "Using image processing techniques and HD-EMG for upper limb prosthesis gesture recognition", *Conf. paper, congress on pattern recognition Springer*, pp 913-921.
- [19] Amma, C Krings, T Boer and J Schultz T, *the 33rd Annual ACM Conference on Human Factors in Computing Systems 2015*, "Advancing muscle-computer interfaces with high-density electromyography", pp. 929–938.
- [20] Du Y, Wenguang J, Wentao W and Geng W: CapgMyo: a high density surface electromyography database for gesture recognition. <http://zju-capg.org/myo/data/index.html>
- [21] H A Jaber, M T Rashid, L Fortuna, 2019, " Robust hand gesture identification using envelope of HD-sEMG signal", *ACM Int. Conf. Proc. Series*.
- [22] H A Jaber, M T Rashid, 2019, "HD-sEMG gestures recognition by SVM classifier for controlling prosthesis", *Iraqi J. of Comp. Commun. Control and Syst. Eng. (IJCCCE)*, vol. 19, No. 1.
- [23] Phinyomark A, Quaine F, Charbonnier S, Serviere C, Tarpin-Bernard Fand Laurillau Y. 2013, "EMG feature evaluation for improving myoelectric pattern recognition robustness" , *Expert Syst. Appl*, vol. 40, pp. 4832–4840.
- [24] Tkach D, Huang H, Kuiken T A, J, 2010, "Study of stability of time-domain features for electromyographic pattern recognition" , *Neuro Eng. Rehab.*, 7, 21.